Galuskin E.V., Kusz J., Galuskina I., Książek M., Vapnik Ye., Zieliński G.

Discovery of terrestrial andreyivanovite, FeCrP, and the effect of Cr and V substitution in barringerite-allabogdanite low-pressure transition.

Supplementary figure

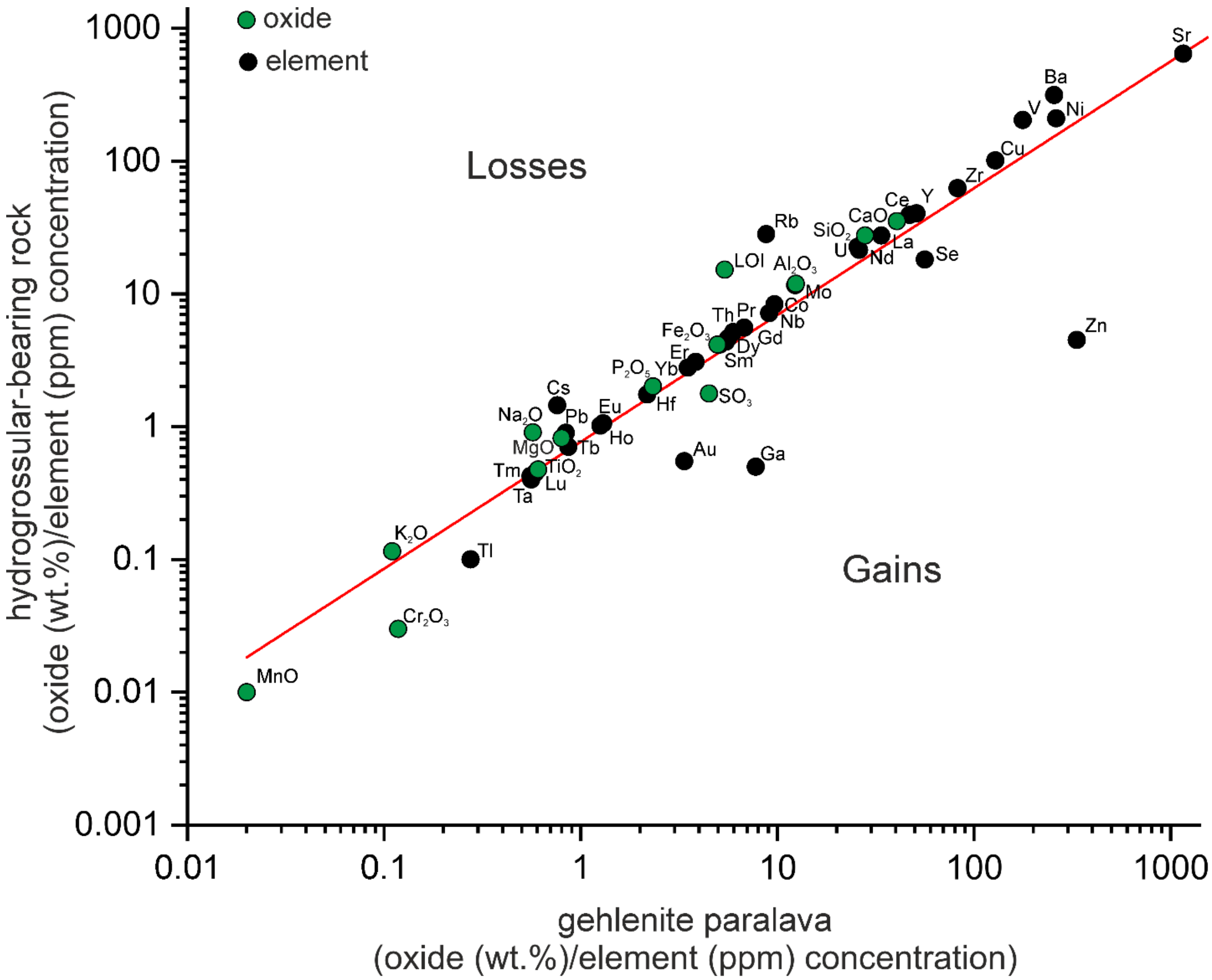

Figure S1

Figure S1. Isocon diagram comparing hydrogrossular-bearing rocks (mean 2 analyses, Table S1) and gehlenite paralava (mean 5, Table S1). Almost all major oxides fall on or near a line. The correlation indicates that there was one type of protolith for both rock types.

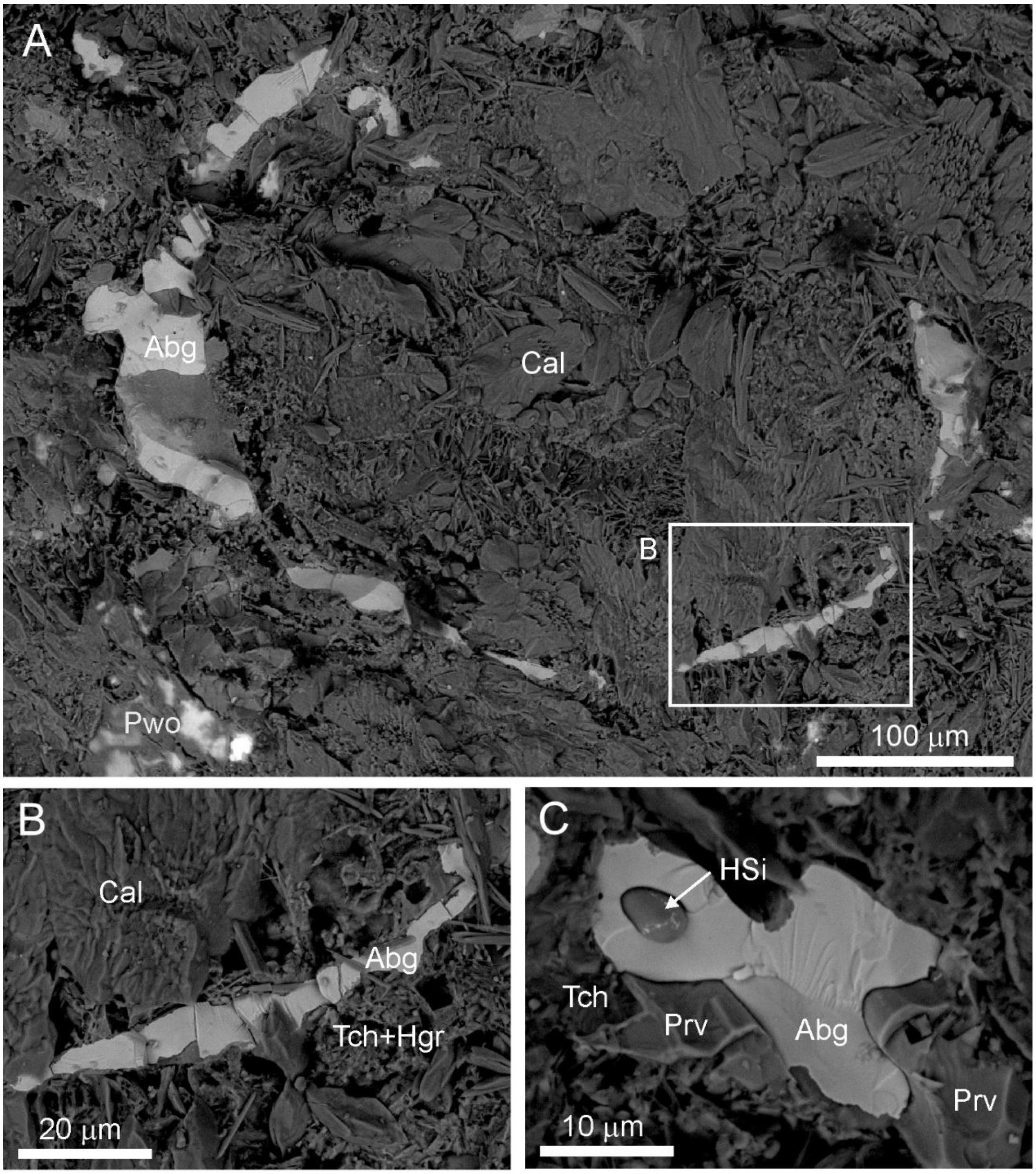

Figure S2

Figure S2. (A) Semi-rounded allabogdanite aggregates in paralava fragment replaced completely by calcite. Natural surface. Frame shows the fragment magnified in Fig. S2B. (B) A part of semi-circle composed of monocrystalline fragments of allabogdanite. (C) Character of pseudomorph surface composed of allabogdanite after fishbone remains. BSE images. Abg = allabogdanite, Cal = calcite, HSi = hydrosilicate, Hgr = hydrogrossular, Prv = perovskite, Pwo = pseudowollastonite, Tch = tacharanite.

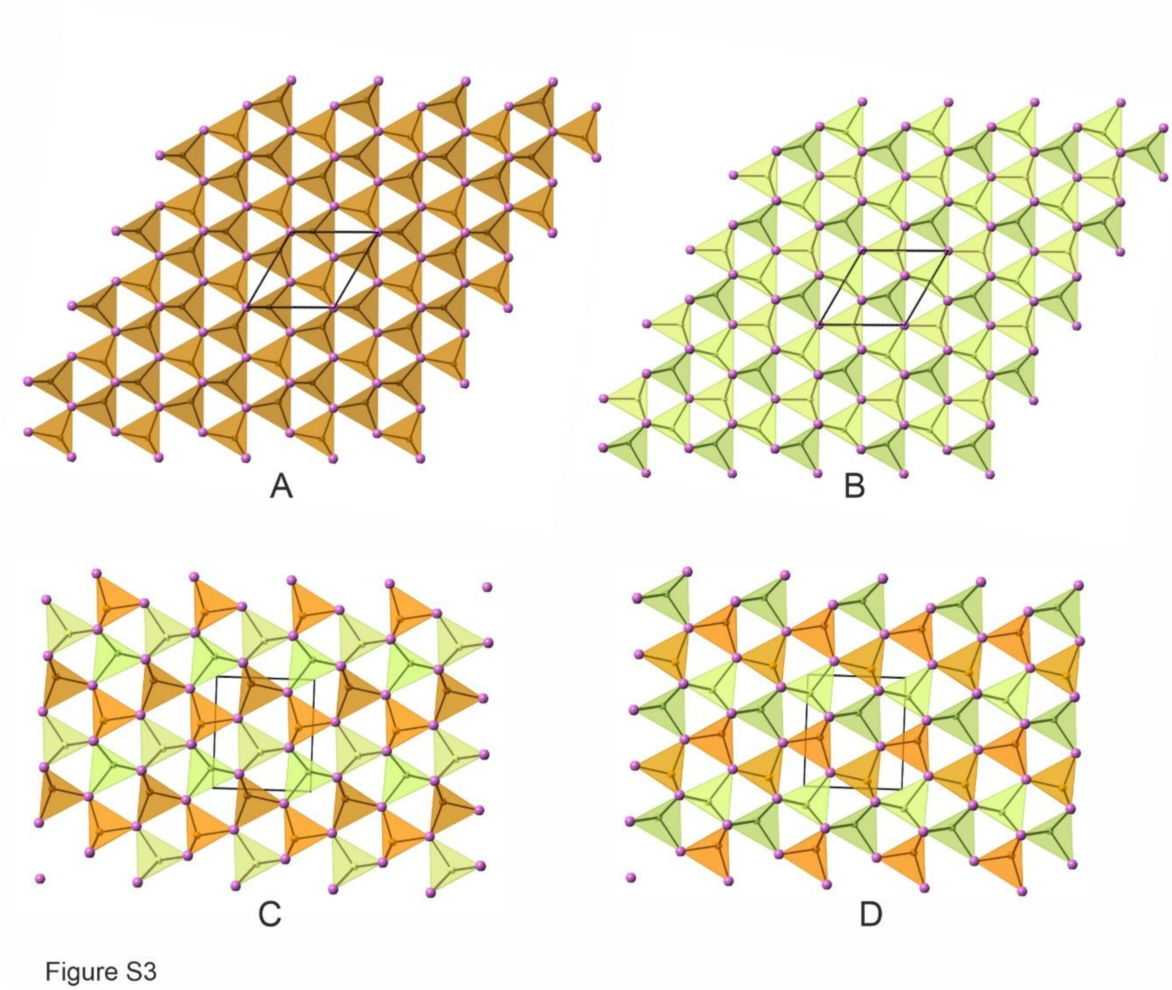

Figure S3. (A,B) Two types of structural layers intercalated in barringerite: (A) layer composed of FeP_4 tetrahedra; (B) layer formed by FeP_5 pyramids. (C, D) One type of structural layer alternately oriented in the opposite direction in the allabogdanite-type structure. Layers are formed by FeP_4 chains of tetrahedra (brown) and FeP_5 chains of pyramids (green).

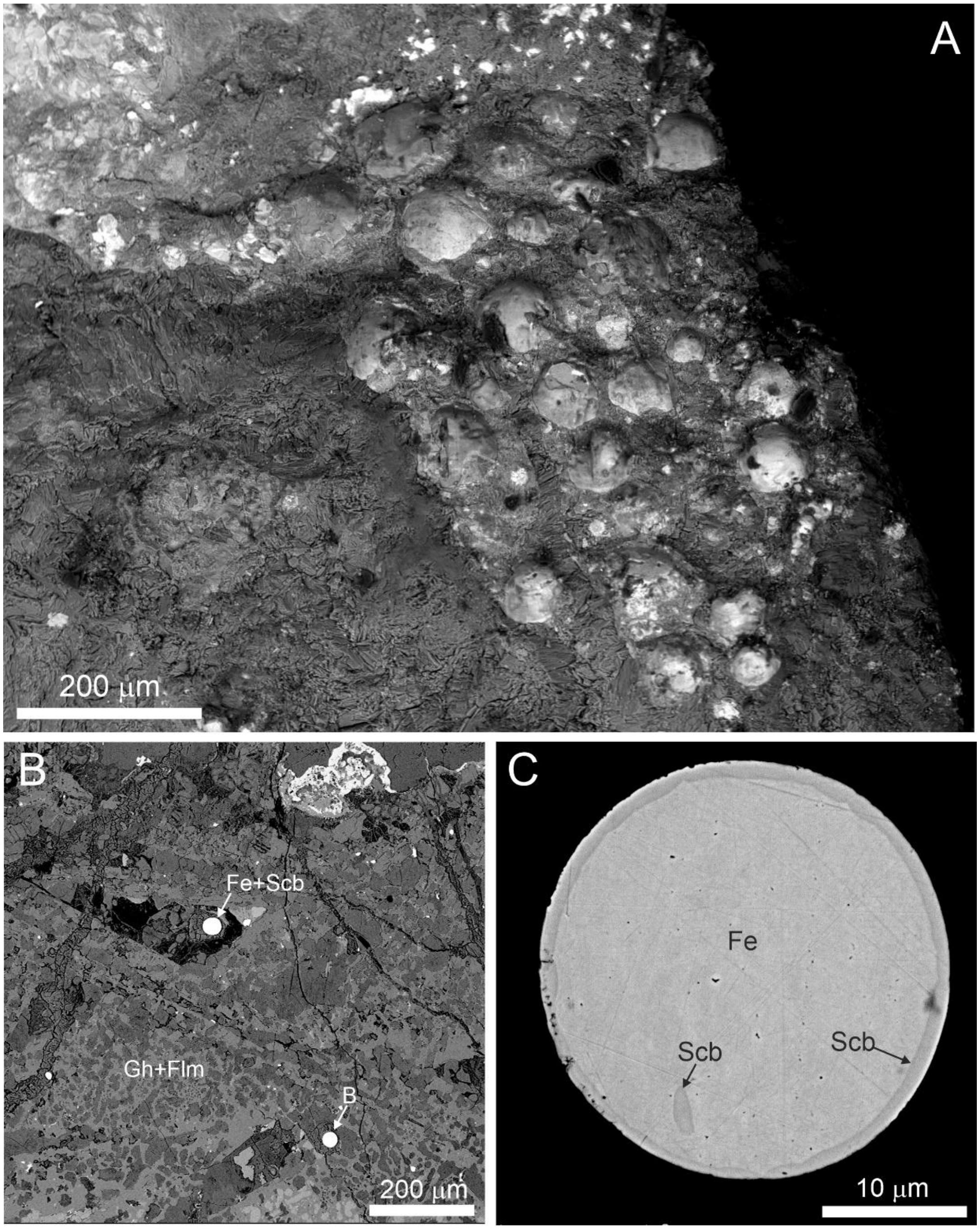

Figure S4

Figure S4. (A) Rounded aggregates of minerals of the Fe-P(±C) system on the boundary of paralava and hydrogrossular rock, in this case, enriched in minerals of the ettringite group (grey), natural surface. (B) Altered gehlenite-flamite paralava with mineral balls of the Fe-P system. Ball marked by letter B is magnified in Fig. S3C. (C) Ball of native iron with schreibersite rim. BSE images. Fe = native iron, Srb = schreibersite, Gh = gehlenite, Flm = flamite.

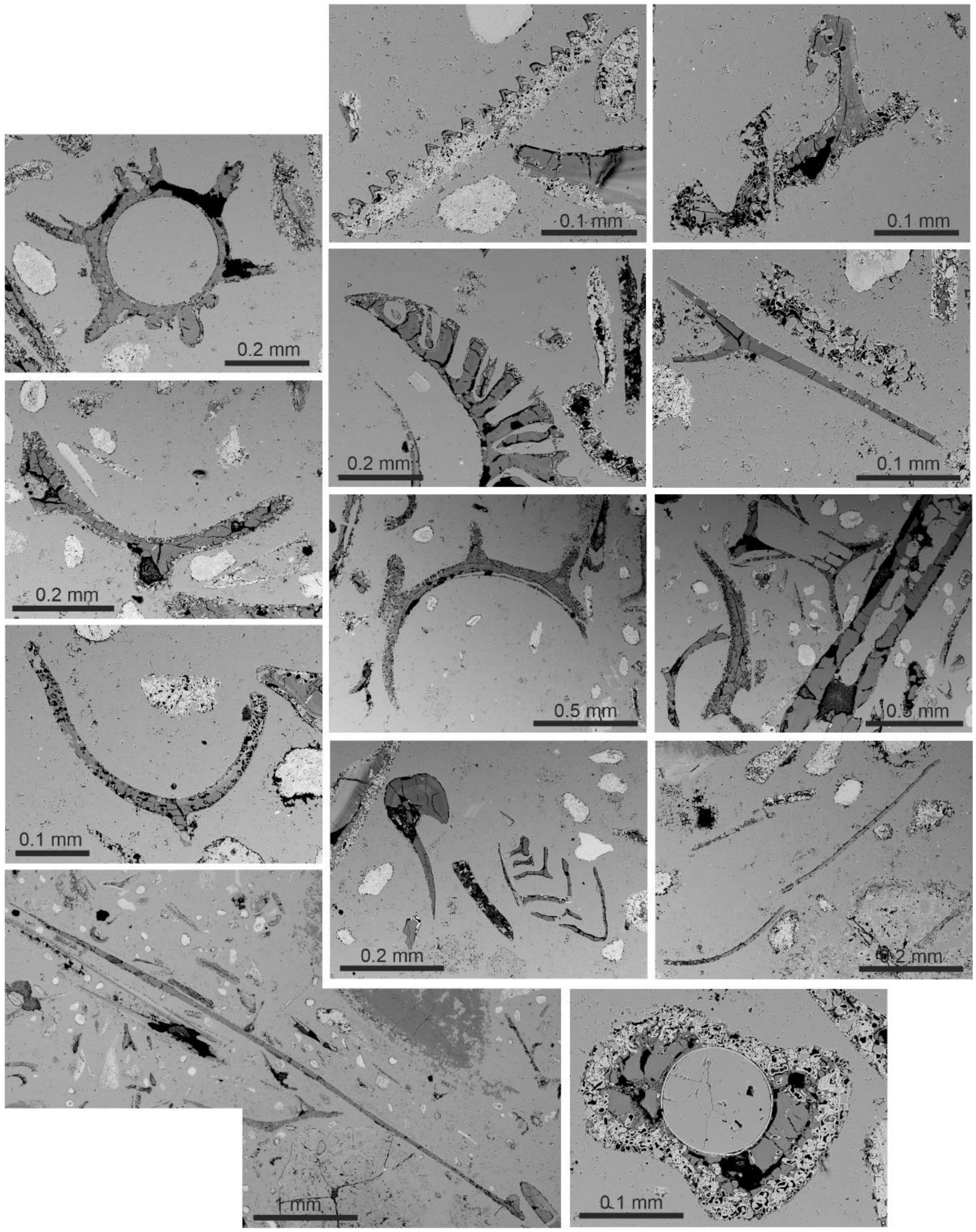

Figure S5

Figure S5. Fishbone remains in phosphorites of the Mishash formation, which underlay rocks of the Ghareb formation, Negev Desert. Grey – carbonate-bearing hydroxylapatite ("francolite") in bone remains, light-grey – calcite, white – newly formed fluorapatite. BSE images.

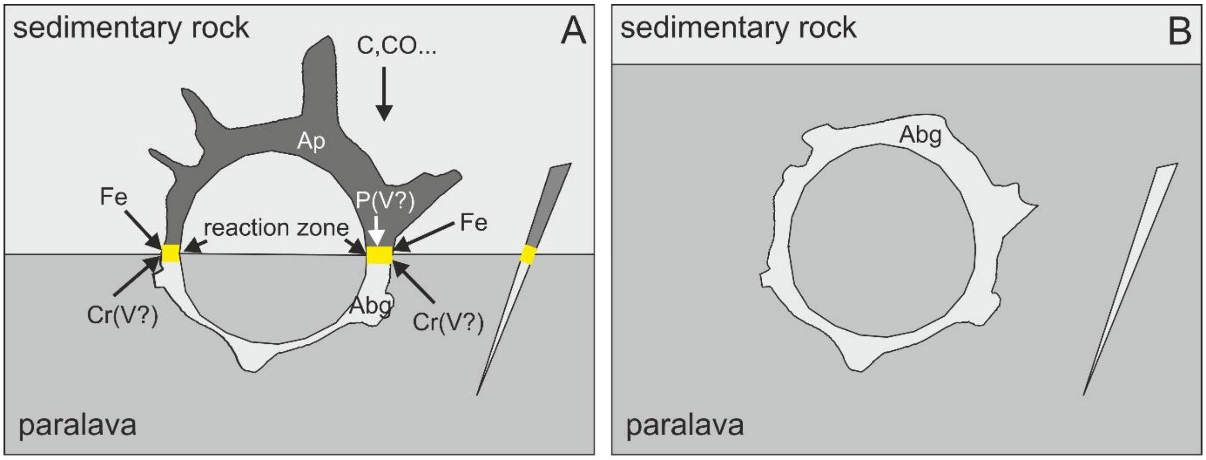

Figure S6

Figure S6. Possible mechanism of pseudomorph formation after fish bone remains. (A) On the boundary of paralava and sedimentary rock replacement of bone remains appear within the reaction zone (shown in yellow). The position of the reaction zone is approximately related to the position of the paralava front. (B) When shifting the paralava front, pseudomorphs after bone remains composed of orthorhombic phosphide of the allabogdanite-andreyivanovite series are preserved by the paralava. Ap = apatite, Abg = allabogdanite.

Table S1. Major oxide and trace element composition (wt% and ppm, respectively) of phosphide-bearing breccia (1-7) and unaltered chalk of Ghareb Formation (8) Hatrurim Basin, Israel.

	1	2	3	4	5	6	7	8
P_2O_5	2.24	2.50	1.98	1.92	3.00	2.00	2.02	0.25
SiO_2	28.53	29.01	26.83	27.44	27.67	27.15	27.89	3.44
TiO_2	0.60	0.63	0.56	0.62	0.63	0.48	0.47	0.05
Al_2O_3	13.13	12.13	12.38	12.35	11.66	11.63	11.66	1.26
Cr_2O_3	0.10	0.12	0.13	0.12	0.12	0.03	0.03	<0.01
Fe_2O_3	5.19	5.41	5.49	4.15	4.58	4.10	4.21	1.24
MgO	0.79	0.86	0.75	0.75	0.85	0.78	0.86	1.06
CaO	38.53	45.62	37.59	39.64	41.14	34.98	35.68	51.00
MnO	0.02	0.02	0.02	0.02	0.02	0.01	0.01	0.05
Na_2O	0.54	0.41	0.73	0.49	0.68	0.87	0.94	0.34
K_2O	0.03	0.27	<0.01	<0.01	0.03	0.13	0.10	<0.01
SO_3	2.866	0.920	6.415	8.152	4.081	1.566	1.994	0.087
LOI	7.67	2.49	6.43	4.91	5.44	16.20	14.24	40.79
Total	100.38	100.55	99.43	100.72	100.01	99.99	100.17	99.57
TOT/C	0.23	0.24	0.21	0.17	0.34	1.82	1.03	10.88
Ba	164	248	526	151	189	441	187	22
Be	<1	2	<1	1	<1	<1	1	<1
Co	9.1	10.5	10.4	8.6	9.7	8.5	8.2	4.9
Cs	1.4	0.2	1.1	0.7	0.4	1.6	1.3	<0.1
Ga	9.8	4.8	8.1	8.4	<0.5	<0.5	<0.5	1.7
Hf	2.1	2.4	2.0	2.2	2.2	1.8	1.7	0.3
Nb	9.7	9.9	7.9	9.0	8.9	7.2	7.1	1.0
Rb	14.2	5.4	10.6	7.1	6.5	29.7	26.6	0.4
Sn	<1	<1	<1	<1	<1	<1	<1	<1
Sr	1212.4	1364.0	973.0	1265.3	985.8	652.8	635.6	633.3
Ta	0.6	0.6	0.5	0.5	0.6	0.4	0.4	<0.1
Th	6.3	6.0	5.7	6.2	5.6	5.2	5.1	0.6
U	25.8	27.3	23.0	24.7	27.2	23.2	22.1	3.7
V	187	184	169	173	171	212	196	33
W	0.8	0.8	0.8	0.8	0.8	0.7	0.6	<0.5
Zr	79.8	90.8	70.4	81.6	89.9	63.7	61.4	11.4
Y	50.0	57.3	45.1	48.6	54.0	41.0	39.8	10.0
La	33.6	36.8	31.0	33.1	34.3	27.2	27.8	6.4
Ce	48.9	50.5	43.1	47.3	45.0	39.2	39.5	7.1
Pr	6.88	7.31	6.18	6.72	6.80	5.54	5.57	1.24
Nd	26.8	27.3	23.8	25.8	26.3	21.4	21.6	5.0
Sm	5.13	5.52	4.78	5.18	4.87	4.15	4.17	0.97
Eu	1.30	1.42	1.20	1.27	1.32	1.08	1.04	0.27
Gd	5.47	6.24	5.18	5.45	5.73	4.63	4.63	1.19
Tb	0.84	0.96	0.81	0.84	0.88	0.71	0.70	0.18
Dy	5.31	5.97	5.05	5.27	5.72	4.40	4.32	1.11
Ho	1.21	1.36	1.16	1.25	1.31	1.01	1.03	0.26
Er	3.67	4.23	3.46	3.81	4.00	3.08	3.06	0.75
Tm	0.53	0.63	0.50	0.55	0.57	0.42	0.43	0.12
Yb	3.39	3.80	3.21	3.41	3.69	2.85	2.71	0.69
Lu	0.56	0.64	0.53	0.58	0.63	0.46	0.44	0.12
Mo	10.1	15.0	15.3	8.4	13.4	11.9	11.9	0.7
Cu	106.0	128.4	149.2	116.5	141.0	98.8	103.2	13.8
Pb	1.0	0.4	0.9	1.0	0.9	1.0	0.8	3.7
Zn	354	113	727	374	95	3	6	32
Ni	210.8	268.3	325.1	214.3	289.4	212.0	207.4	26.9
As	<0.5	2.5	<0.5	<0.5	<0.5	4.2	6.8	1.7
Cd	<0.1	<0.1	<0.1	<0.1	<0.1	<0.1	<0.1	0.3
Sb	<0.1	0.1	<0.1	<0.1	<0.1	0.3	0.2	0.2
Bi	<0.1	<0.1	<0.1	<0.1	<0.1	<0.1	<0.1	<0.1
Ag	0.5	0.3	0.6	0.8	0.6	0.1	0.1	<0.1
Au	4.1	2.4	3.1	2.9	4.3	0.6	<0.5	2.2
Hg	<0.01	<0.01	<0.01	<0.01	0.01	0.03	0.02	<0.01
Tl	0.4	<0.1	0.3	0.2	0.2	<0.1	<0.1	<0.1
Se	33.2	7.9	>100.0	>100.0	39.6	19.4	16.9	<0.5

1 – black gehlenite paralava with small amygdules; 2 – gehlenite paralava with amygdules filed with ettringite; 3 – gehlenite paralava with flow structure, porous; 4 – gehlenite paralava without visible pores; 5 - black gehlenite paralava, inhomogeneous; 6 - fragment of country rock, grey, not massive; 7 - fragment of country rock, grey-pinkish, massive; 8 – chalk

Table S2. Data collection and structure-refinement details for Cr-V-bearing phosphides

Group number/grain number		1b/23	1a/18	2/3	2/7	2/9	3/61	4a/1	4b/62	4c/68	5/64
Crystal system			hexagonal					orthorhombic			
Unit cell dimensions (Å)	*a*	5.8588(3)	5.8565(3)	5.8414(3)	5.8003(3)	5.8020(2)	5.8165(4)	5.8269(4)	5.8307(3)	5.8269(6)	5.8231(3)
	b	5.8588(3)	5.8565(3)	5.8414(3)	3.5665(3)	3.56639(14)	3.5664(2)	3.5689(3)	3.5645(2)	3.5624(4)	3.5666(2)
	c	3.4673(2)	3.47116(19)	3.4922(2)	6.6405(4)	6.6448(3)	6.6531(4)	6.6627(5)	6.6617(4)	6.6599(8)	6.6564(3)
	α		90°					90°			
	β		90°					90°			
	γ		120°					90°			
Space group			*P-6 2 m* (168)					*P n m a* (62)			
Volume (Å^3)		103.070(12)	103.106(12)	103.197(14)	137.371(15)	137.496(10)	138.015(15)	138.556(19)	138.452(14)	138.24(3)	138.243(13)
Z			3					4			
Density (calculated) g/cm^3		6.860	6.855	6.790	6.811	6.811	6.745	6.706	6.644	6.674	6.674
Crystal size (nm)		30×20×20	40×25×20	40×40×20	22×20×16	40×40×16	30×20×12	28×18×10	45×20×20	20×20×12	28×25×12
Data collection											
Diffractometer							SuperNova MoKα 0.71073 293(2)				
X-ray power							50 kV, 0.8 mA				
Detector							Atlas CCD (Agilent Technologies)				
Max. θ range for data collection (°)		26.139	26.141	26.337	26.347	26.331	26.296	26.346	26.348	26.357	26.372
Index ranges		-7<*h*<7	-7<*h*<5	-6<*h*<7	-7<*h*<7	-7<*h*<7	-6<*h*<7	-5<*h*<7	-7<*h*<7	-7<*h*<7	-7<*h*<6
		-7<*k*<7	-7<*k*<7	-7<*k*<6	-3<*k*<4	-4<*k*<4	-4<*k*<4	-4<*k*<4	-3<*k*<4	-4<*k*<4	-3<*k*<4
		-3<*l*<4	-4<*l*<4	-4<*l*<3	-8<*l*<8	-7<*l*<8	-8<*l*<8	-7<*l*<8	-8<*l*<8	-8<*l*<5	-8<*l*<8
No. of measured reflections		844	842	904	1054	2034	1027	1019	1022	969	1014
No. of unique reflections		99	99	101	166	166	166	167	167	166	167
Refinement of the structure											
no. of parameters		15	15	15	20	20	20	20	20	20	20
R_{int}		0.0185	0.0216	0.0198	0.0194	0.0168	0.0230	0.0258	0.0150	0.0266	0.0180
$R1_{(obs)}$ / $R1_{(all)}$		0.0121/0.0122	0.0116/0.0121	0.0183/0.0183	0.0142/0.0152	0.0192/0.0193	0.0232/0.0240	0.0469/0.0487	0.0117/0.0122	0.0151/0.0174	0.0283/0.0287
$wR2_{(obs)}$ / $wR2_{(all)}$		0.0308/0.0308	0.0294/0.0295	0.0443/0.0443	0.0326/0.0330	0.0500/0.0501	0.0575/0.0580	0.1235/0.1250	0.0289/0.0294	0.0363/0.0378	0.0747/0.0753
$GOF_{(obs)}$ /$GOF_{(all)}$		1.221	1.269	1.195	1.125	1.189	0.894	1.106	0.881	0.893	1.066
Δρ min. (-e. Å^{-3})		-0.370	-0.384	-0.985	-0.432	-0.802	-0.561	-0.850	-0.606	-0.822	-0.809
Δρ max. (e. Å^{-3})		0.321	0.449	0.719	0.464	0.748	1.429	3.325	0.481	0.589	1.450

Table S3a. Atom coordinates, *U*eq (Å^2) and anisotropic displacement parameters *U*ij for barringerite grains

	site	atom	*x/a*	*y/b*	*z/c*	U^{eq}	*sof*	U^{11}	U^{22}	U^{33}	U^{23}	U^{13}	U^{12}
1a/18	Fe1	Fe	0.25659(17)	0.25659(17)	0	0.0048(3)	1	0.0032(5)	0.0032(5)	0.0076(6)	0	0	0.0014(5)
	Fe2	Fe	0.4055(3)	0	0.5	0.0062(4)	0.986(5)	0.0054(5)	0.0082(6)	0.0058(6)	0	0	0.0041(3)
	P1	P	0	0	0.5	0.0056(7)	1	0.0060(11)	0.0060(11)	0.0050(14)	0	0	0.0030(5)
	P2	P	0.333333	0.666667	0	0.0048(5)	1	0.0038(7)	0.0038(7)	0.0068(11)	0	0	0.0019(4)
1b/23	Fe1	Fe	0.25700(18)	0.25700(18)	0	0.0044(3)	1	0.0034(5)	0.0034(5)	0.0060(5)	0	0	0.0013(5)
	Fe2	Fe	0.4056(3)	0	0.5	0.0059(4)	0.987(5)	0.0053(5)	0.0082(6)	0.0050(6)	0	0	0.0041(3)
	P1	P	0	0	0.5	0.0051(7)	1	0.0061(11)	0.0061(11)	0.0031(12)	0	0	0.0030(5)
	P2	P	0.333333	0.666667	0	0.0046(5)	1	0.0040(7)	0.0040(7)	0.0057(10)	0	0	0.0020(4)
2/3	Fe1	Fe	0.2557(2)	0.2557(2)	0	0.0033(5)	1	0.0025(6)	0.0025(6)	0.0047(7)	0	0	0.0011(5)
	Fe2	Fe	0.4065(3)	0	0.5	0.0053(5)	0.964(7)	0.0049(7)	0.0071(8)	0.0046(8)	0	0	0.0036(4)
	P1	P	0	0	0.5	0.0043(9)	1	0.0053(13)	0.0053(13)	0.0024(14)	0	0	0.0026(7)
	P2	P	0.333333	0.666667	0	0.0039(6)	1	0.0028(8)	0.0028(8)	0.0061(11)	0	0	0.0014(4)

Table S3b. Atom coordinates, *U*eq (Å^2) and anisotropic displacement parameters *U*ij for grains of allabogdanite-andreyivanovite series

	site	atom	*x/a*	*y/b*	*z/c*	U^{eq}	*sof*	U^{11}	U^{22}	U^{33}	U^{23}	U^{13}	U^{12}
2/7	Fe1	Fe	0.14394(9)	0.25	0.56301(8)	0.0036(2)	1	0.0033(3)	0.0046(3)	0.0028(3)	0	-0.0002(2)	0
	Fe2	Fe	0.02798(10)	0.25	0.16746(9)	0.0051(2)	0.968(3)	0.0047(3)	0.0064(3)	0.0041(3)	0	0.0002(2)	0
	P	P	0.76286(17)	0.25	0.62352(16)	0.0040(2)	1	0.0038(4)	0.0049(5)	0.0033(5)	0	0.0014(4)	0
2/9	Fe1	Fe	0.14391(12)	0.25	0.56296(11)	0.0032(3)	1	0.0033(4)	0.0030(4)	0.0032(4)	0	-0.0003(3)	0
	Fe2	Fe	0.02793(14)	0.25	0.16736(12)	0.0052(3)	0.971(5)	0.0058(5)	0.0050(5)	0.0049(4)	0	-0.0002(3)	0
	P	P	0.7629(2)	0.25	0.6235(2)	0.0034(4)	1	0.0037(6)	0.0035(7)	0.0030(7)	0	0.0010(5)	0
3/61	Fe1	Fe	0.14393(13)	0.25	0.56266(13)	0.0038(3)	1	0.0044(5)	0.0031(5)	0.0038(5)	0	-0.0004(3)	0
	Fe2	Fe	0.02765(15)	0.25	0.16771(14)	0.0057(4)	0.956(5)	0.0067(5)	0.0049(5)	0.0055(5)	0	-0.0002(3)	0
	P	P	0.7639(2)	0.25	0.6241(2)	0.0037(4)	1	0.0046(7)	0.0029(8)	0.0037(8)	0	0.0005(6)	0
4a/1	Fe1	Fe	0.1441(2)	0.25	0.5623(2)	0.0054(7)	1	0.0053(10)	0.0035(10)	0.0074(10)	0	-0.0008(6)	0
	Fe2	Fe	0.0273(3)	0.25	0.1682(3)	0.0081(8)	0.950(8)	0.0093(11)	0.0056(11)	0.0095(10)	0	-0.0011(6)	0
	P	P	0.7643(4)	0.25	0.6244(4)	0.0046(8)	1	0.0034(14)	0.0043(15)	0.0061(15)	0	0.0002(10)	0
4b/62	Fe1	Fe	0.14417(6)	0.25	0.56197(6)	0.00296(17)	1	0.0030(2)	0.0033(2)	0.0026(2)	0	0.00000(14)	0
	Fe2	Fe	0.02717(7)	0.25	0.16875(7)	0.00420(18)	0.925(2)	0.0039(3)	0.0050(3)	0.0037(2)	0	0.00010(15)	0
	P	P	0.76492(12)	0.25	0.62441(11)	0.0035(2)	1	0.0036(3)	0.0034(4)	0.0035(4)	0	0.0009(3)	0
4c/68	Fe1	Fe	0.14409(9)	0.25	0.56212(9)	0.0028(2)	1	0.0026(3)	0.0031(3)	0.0027(3)	0	0.0002(2)	0
	Fe2	Fe	0.02708(10)	0.25	0.16866(9)	0.0042(2)	0.933(3)	0.0037(4)	0.0043(4)	0.0046(4)	0	0.0001(2)	0
	P	P	0.76478(16)	0.25	0.62465(17)	0.0034(3)	1	0.0034(5)	0.0031(5)	0.0037(5)	0	0.0004(4)	0
5a/64	Fe1	Fe	0.14420(13)	0.25	0.56210(13)	0.0026(4)	1	0.0027(6)	0.0029(6)	0.0023(6)	0	-0.0003(3)	0
	Fe2	Fe	0.02712(16)	0.25	0.16849(15)	0.0044(4)	0.933(4)	0.0049(7)	0.0045(6)	0.0040(6)	0	-0.0008(3)	0
	P	P	0.7644(2)	0.25	0.6245(2)	0.0028(5)	1	0.0028(8)	0.0031(8)	0.0024(8)	0	0.0006(6)	0

Table S4A. Selected interatomic distances (Å) for barringerite

Atom	-atom	1a/18	1b/23	2/3
Fe1	P1	2.2957(7)×2	2.2962(7)×2	2.2977(8)×2
	P2	2.2114(7)×2	2.2107(7)×2	2.2092(8)×2
mean		2.2536	2.2535	2.2535
Fe2	P1	2.3749(16)	2.3765(16)	2.374(2)
	P2	2.4853(4)×4	2.4843(4)×4	2.4882(4)×4
mean		2.4632	2.4627	2.4654

Table S4B. Selected interatomic distances (Å) for allabogdanite (1-6) and andreyivanovite (7)

		1	2	3	4	5	6	7
Atom	-atom	2/7	2/9	3/61	4a/1	4b/62	4c/68	5/64
Fe1	P	2.1929(12)	2.1945(15)	2.1979(18)	2.202(3)	2.2047(8)	2.2014(13)	2.2006(17)
	P	2.2375(7)×2	2.2379(9)×2	2.2385(11)×2	2.240(2)×2	2.2358(5)×2	2.2365(8)×2	2.2373(11)×2
	P	2.2466(11)	2.2473(14)	2.2479(16)	2.251(3)	2.2500(8)	2.2491(11)	2.2500(16)
mean		2.2286	2.2294	2.2307	2.233	2.2316	2.2309	2.2313
Fe2	P	2.3643(11)	2.3652(15)	2.3784(17)	2.389(3)	2.3949(8)	2.3946(12)	2.3902(18)
	P	2.4721(8)×2	2.4720(11)×2	2.4779(11)×2	2.481(2)×2	2.4828(5)×2	2.4801(8)×2	2.4796(11)×2
	P	2.5648(8)×2	2.5659(11)×2	2.5630(12)×2	2.563(2)×2	2.5582(6)×2	2.5570(9)×2	2.5598(12)×2
mean		2.4876	2.4882	2.4920	2.4954	2.4954	2.4938	2.4938